Organic Electronics 14 (2013) 389–395

Contents lists available at SciVerse ScienceDirect

Organic Electronics

journal homepage: www.elsevier.com/locate/orgel

Preparation and time-resolved fluorescence study of RGB organic crystals

Hong-Hua Fang [a], Shi-Yang Lu [b], Lei Wang [a], Ran Ding [a], Hai-Yu Wang [a], Jing Feng [a,*], Qi-Dai Chen [a], Hong-Bo Sun [a,b,*]

[a] State Key Laboratory on Integrated Optoelectronics, College of Electronic Science and Engineering, Jilin University, 2699 Qianjin Street, Changchun 130012, People's Republic of China
[b] College of Physics, Jilin University, 119 Jiefang Road, Changchun 130023, People's Republic of China

ARTICLE INFO

Article history:
Received 4 September 2012
Received in revised form 13 October 2012
Accepted 14 October 2012
Available online 9 November 2012

Keywords:
Organic crystals
Tunable photoluminescence
RGB emission: ultrafast spectroscopy
Energy transfer
Exciton–exciton annihilation

ABSTRACT

In this work, large-size tetracene- and pentacene-doped 1,4-Bis(4-methylstyryl)-benzene (BSB-Me) crystals were prepared with physical vapor transfer technique. The photoluminescence emission can be adjusted from blue to green and even to red by changing the doping. Their fluorescence features are investigated by both the steady-state fluorescence spectra and time-resolved fluorescence measurements, which indicate highly efficient energy transfer from the host BSB-Me to the acceptor. The PL efficiencies of the tetracene-doped BSB-Me and pentacene-doped BSB-Me crystals are as high as 79% and 47%, the energy transfer efficiency is 49.7% and 73.1%, respectively. Excitation intensity-dependent ultrafast dynamics was further probed, which shows that the kinetics in doped crystals exhibit much less excitation intensity dependence than that of the pure BSB-Me crystals. Our results are relevant to the understanding of ultrafast energy-transfer dynamics in doped crystals and are expected to be of interest for organic light emitting transistors, diodes, and lasers.

1. Introduction

Organic thin films with advanced functions have attracted the world's attention for decades from academic research to industrial application [1–4]. Conceptually, organic materials allow chemical engineering of electronic and photonic properties by molecular design, taking advantage of low cost, flexibility and low temperature processing [5–9]. Organic optoelectronic thin films exhibit high sensitivity to electrical and optical stimulus and can realize light-emitting diode (OLED) and other extremely promise applications, such as transistors, photovoltaics and compact laser systems [10–14]. For producing reliable high-quality devices, the preferred organic semiconductor must be well ordered and stable with closely-packed molecules having few defects between molecules or domains. The long-range order presented in thin films of crystalline organic semiconductors results in high charge carrier mobility and some of the crystals exhibit high luminescence efficiency making them superior in electronic and optical performance [8,10–19]. Enormous recent efforts have brought significant progresses in the growth of organic single crystals, the fabrication of single crystal devices and the investigation of structure–properties relationship of organic semiconductors based on the crystals [8,11,16,19–27].

To achieve multi-color displays and to meet the need of next generation light-emitting materials, it is important to tune and control the luminescent color of an organic material [7,28–30]. Doping has been proven to be an efficient way to tune the emission color of fluorescent materials [31–33]. It is widely applied in the field of inorganic crystalline materials and organic thin film systems. However, as compared with extensive investigation of inorganic

* Corresponding authors at: State Key Laboratory on Integrated Optoelectronics, College of Electronic Science and Engineering, Jilin University, 2699 Qianjin Street, Changchun 130012, People's Republic of China. Tel./fax: +86 431 85168281.
E-mail addresses: jingfeng@jlu.edu.cn (J. Feng), hbsun@jlu.edu.cn (H.-B. Sun).

1566-1199/$ - see front matter Crown Copyright © 2012 Published by Elsevier B.V. All rights reserved.
http://dx.doi.org/10.1016/j.orgel.2012.10.028

doped crystals or organic thin films, little attention has been paid on doping in organic crystals. Weak intermolecular interactions between host and guest molecules in organic crystals make them fundamentally different from their inorganic counterparts, doping in organic crystals still poses a technological challenge. Recently, several works focused on doping in organic crystals as well as their applications in photoelectric devices have been reported. For example, Yao and coworkers developed tunable fluorescence emission 1,3,5-triphenyl-2-pyrazoline (TPP) nanoparticles doped with 4-(dicyanomethylene)-2-methyl-6-(p-dimethylaminostyryl)-4H-pyran (DCM) [34] and white-light-emitting TPP nanowires doped with rubrene [35]; Xu et al. reported tetracene-doped anthracene nanowire arrays [32]; Ma's research team realized wavelength tunable amplified spontaneous emission in crystals [28]. Most of these molecular crystals are small in size (usually at the micro/nanoscale) [32–34,36,37]. Large size crystals with color-tunable emission, which are high demand for fabrication of devices, are rare. On the other hand, the exciton recombination dynamics and energy transfer may be greatly affected by the introduction of doping materials. Many basic aspects of these issues have not been well addressed yet in the organic crystals. Thus, achieving desirable light emission and understanding the energy transfer in doped organic crystal are significant towards organic electroluminescence and photonic applications.

In this paper, tetracene- and pentacene-doped 1,4-Bis(4-methylstyryl)benzene (BSB-Me) crystals with high crystalline quality, and excellent optical properties have been successfully prepared by physical vapor transport technique. The fluorescence can be tuned from blue to green and even to red (blue for the undoped BSB-Me, blue-green to green for the tetracene-doped BSB-Me and red for the pentacene doped BSB-Me crystals). These doped crystals have large sizes (several millimeters), high luminescent efficiency (91% for the undoped BSB-Me, 79% for the tetracene-doped BSB-Me, and 47% for the pentacene-doped BSB-Me crystals). Ultrafast fluorescence dynamics of undoped and doped crystals are investigated by nanosecond fluorescence lifetime experiments and sub-picosecond time-resolved upconversion method to resolve the energy transfer from the host to the guest and the suppressing of the interaction among the guest molecules.

2. Experimental section

2.1. Growth of crystals

1,4-Bis(4-methylstyryl)benzene (BSB-Me) powder was purchased from Tokyo Chemical Industry Co., Ltd., and tetracene, pentacene powder were supplied by Alfa Aesar Co., Ltd. Their chemical structures are listed in Fig. 2a. Before crystal growth, the tetracene (or pentacene) and BSB-Me powders (2 and 20 mg, respectively) were simultaneously milled in a mortar for a few minutes, resulting in the formation of the uniform mixed powder, and subsequently put into a quartz boat. All organic crystals were grown by a physical vapor transport method using the mixed powder. The apparatus for the preparation of the crystals are very similar with that reported in the literature [16], as displayed in Fig. 1. The growth method used two heating zones in a horizontal tube furnace. The quartz boat loaded with the mixture was then put into the center of a quartz tube, which was inserted into the high temperature zone of the tube furnace. The high-purity argon was adopted as carrier and to prevent the materials from being oxidized. The gas flowing rate was kept at 50 mL/min. A temperature $T_s = 270\ ^\circ C$ was maintained at the material source, and crystal growth region was $T_g = 240\ ^\circ C$ for growth of both tetracene-doped and pentacene-doped BSB-Me crystals. These temperature conditions for crystal growth were almost the same as for single crystals of pure BSB-Me. The thin plate-like crystals obtained have typical thickness of range from hundreds nanometers to several micrometers and a length of a few millimeters.

2.2. Optical measurements and XRD measurements

The top-view photographs of organic crystals under UV-light irradiation were observed using the optical microscope. The PL characteristics of the crystals were measured on a spectrophotometer (AvaSpec 2048-UA-50-AF spectrometer). Quantum yield of photoluminescence Φ_{PL} were measured using an integrating sphere (C-701, Labsphere Inc.), with a 405 nm Ocean Optics LLS-LED as the excitation source, and the laser was introduced into the sphere through the optical fiber. XRD patterns were recorded using a Rigaku X-ray diffractometer (D/max-rA, using Cu Kα radiation of wavelength 1.542 Å). Standard scans were acquired from 5° to 60° (2θ).

2.3. Time-resolved fluorescence spectroscopy

Nanosecond fluorescence lifetime experiments were performed by a time-correlated single photon counting (TCSPC) system under right-angle sample geometry. A 405 nm picosecond diode laser (Edinburgh Instruments EPL405) was used to excite the samples. The fluorescence was detected by a photomultiplier tube (Hamamatsu H5783p), which is connected to a TCSPC board (Becker&Hickel SPC-130).

Sub-picosecond time resolved emission was carried out with a femtosecond fluorescence up-conversion technique, the details of which are described elsewhere. Briefly, a mode-locked Ti:sapphire laser/amplifier system (Solstice, SpectraPhysics) was used. The output of the amplifier of 1.5-mJ pulse energy, 100 fs pulse width, at 800 nm wavelength is split into two equal parts; the second harmonic (400 nm) of one beam was focused in the sample as excitation. The resulted fluorescence was collected and focused onto a 1 mm thick BBO crystal with a cutting angle of 35°. The other part of the RGA output was sent into an optical delay line and served as the optical gate for the upconversion of the fluorescence. The generated sum frequency light was then collimated and focused into the entrance slit of a 300 mm monochromator. A UV-sensitive photomultiplier tube 1P28 (Hamamatsu) was used to detect the signal.

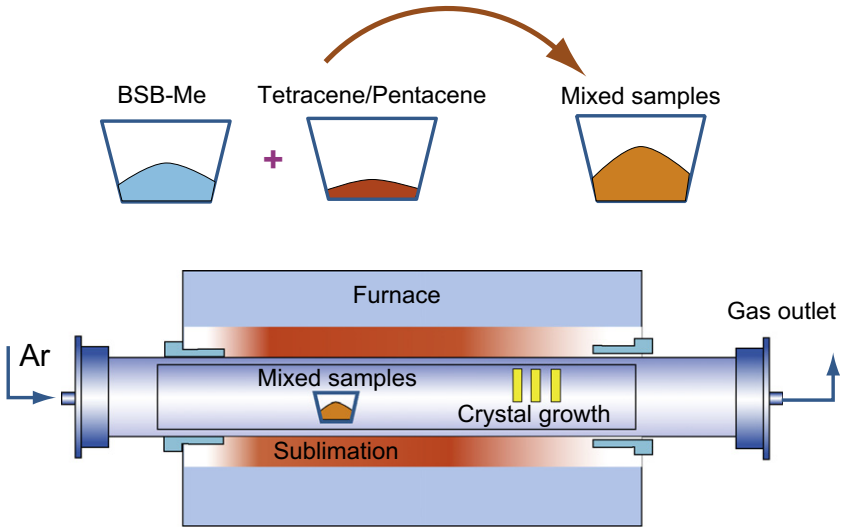

Fig. 1. Schematic diagrams of the experimental setup for doped crystal growth. Before crystal growth, the doping and BSB-Me powders were simultaneously milled in a mortar for a few minutes, resulting in the formation of the uniform mixed powder.

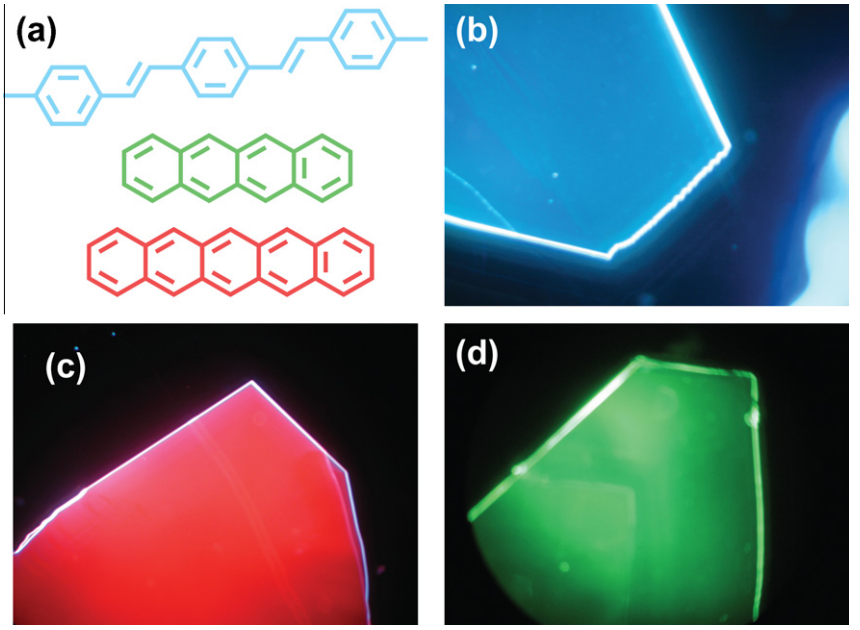

Fig. 2. (a) The molecular structures of BSB-Me, tetracene, pentacene. (b) The pure BSB-Me crystal. (c) Pentacene doped BSB-Me crystal. (d) Tetracene-doped BSB-Me crystal photographs under the ultraviolet lamp.

3. Results and discussions

3.1. Molecular ordering

Fig. 2b–d shows top-view photographs of the pure BSB-Me, tetracene- and pentacene-doped BSB-Me crystals with PL under fluorescence microscopic observation. The doped crystals have the slice shape, smooth surface, and large size of several millimeters as similar as pure BSB-Me crystal. To investigate the molecular ordering of the doped crystals, X-ray diffraction (XRD) spectra of pure BSB-Me, tetracene-doped BSB-Me, and pentacene-doped crystals were measured. Fig. 3 shows the out-of-plane XRD spectra of these crystals. From the diffraction peak of the BSB-Me single crystal at 2θ of 13.66° (006). The thickness of one molecular layer is calculated to be 1.86 nm, corresponding to the spacing of the *c*-axis. It indicates that the long axis of the molecules is ordered perpendicular to the wide crystal face and the *ab*-plane is parallel to the substrate. Compared to pure BSB-Me, the doped crystal did not change so much.

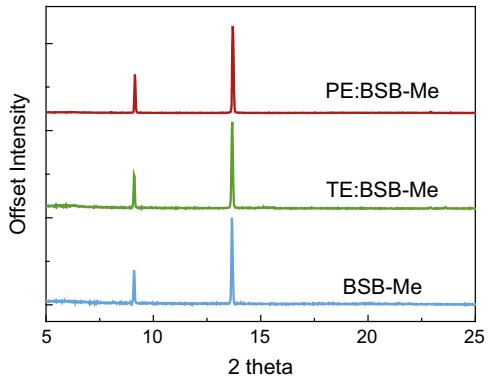

Fig. 3. XRD pattern of pure BSB-Me, tetracene- and pentacene-doped crystals.

The diffraction pattern of the doped crystal did not show any diffraction peaks consistent with a tetracene or a pentacene single crystal, indicating that the doping molecules did not form aggregated domain structures in the BSB-Me crystal. The diffraction peak of the tetracene-doped BSB-Me crystal appeared at 2θ of 13.68° and of the pentacene-doped BSB-Me crystal appeared at 2θ of 13.70°, which are a very similar spacing to that of the pure BSB-Me crystal. No significant changes induced by doping molecules were observed in the crystal structure. From the parameters, we can find that similar layer-by layer structures formed in doped system and the doped effect is not strong enough to disorder the domain structure. For the host and guest molecules, they are all the linear configurations. Both tetracene and pentacene are polycyclic aromatic hydrocarbons composed of linearly fused benzene rings, with tetracene and pentacene composed of 4 and 5 benzene rings, respectively. Their sizes are smaller than that of the host molecules BSB-Me. It means that tetracene and pentacene molecules can fill in the defects or vacancies of the crystal lattice without distortion. Furthermore, the ratio between the guest and host was very small, which is less than 1:20. In other word, there is less than one dopant per twenty host molecules in the doped crystals. The number is not high enough to change the host crystal structures. In physical vapor transport process, host and guest molecules could freely diffuse onto the crystal surface from vapor, and then may combine with neighboring molecules through intermolecular interactions to form an intact layer. The doping molecules were dispersed throughout the BSB-Me host crystal lattice, and a certain quantity of doped guest molecules may replace the locations of original host molecules in the crystal lattice.

3.2. PL characteristics

Although strong blue[1] emission from the pure BSB-Me crystal was clearly observed (Fig. 2b), the emission color could be tuned to be green or red by doping with tetracene or pentacene, respectively (Fig. 2c and d). Fig. 4 shows a steady-state fluorescence spectrum of crystals (BSB-Me, tetracene:BSB-Me and pentacene:BSB-Me), which were photo-excited with a 405 nm lasers, and absorption spectra of tetracene and pentacene in tetrahydrofuran solution. The obtained spectrum for BSB-Me/tetracene crystal exhibits vibrational structures at 470, 495, 530, 570, and 620 nm. We note that there is an overlap in spectrum between pure and tetracene-doped crystal. It indicates that the energy transfer of singlet excitons from BSB-Me donor molecules to tetracene acceptor molecules occurs incompletely. The pentacene-doped crystal exhibits emission peaks at 605, 655, and 716 nm, and the emission peaks of BSB-Me are almost suppressed. It implies high energy transfer efficiency between BSB-Me and pentacene, and nearly all excitation energy of BSB-Me is transferred to pentacene molecules. The herringbone arrangement of tetracene and pentacene molecules in their solid-state can quench the luminescence sharply, so their luminescent efficiencies in the aggregated state (crystals) are no more than 1%. But doping tetracene or pentacene into a host crystal could effectively avoid the intermolecular aggregates. The crystalline-state PL efficiencies of the tetracene-doped BSB-Me and pentacene-doped BSB-Me crystals are as high as 79% and 47%, respectively.

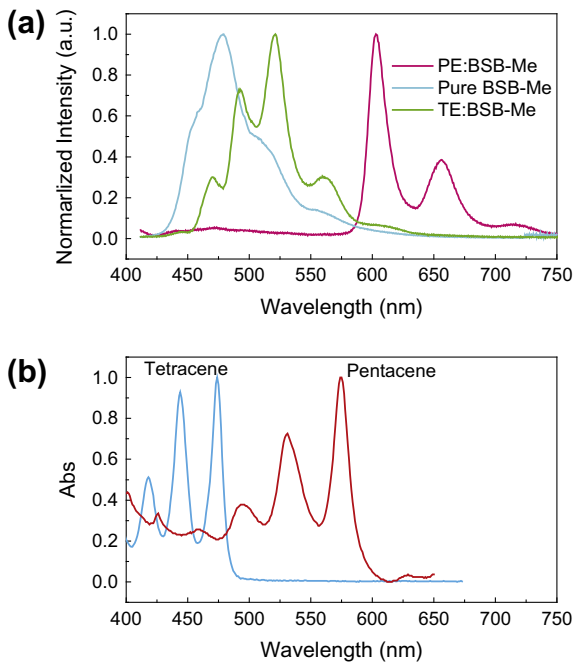

Fig. 4. (a) Emission spectra of pure, tetracene, and pentacene doped crystals. (b) Absorption spectroscopy of tetracene and pentacene in tetrahydrofuran solution.

3.3. Fluorescence dynamics in doped crystal

The photoluminescence of doped crystals have been modulated through the introduction of doping in BSB-Me crystals. Because of the spectral overlapping between donors and acceptors, the donor centers can relax either by direct energy transfer to acceptors (nonradiative energy transfer) or by first radiative recombination in the donor

[1] For interpretation of color in Fig. 2, the reader is referred to the web version of this article.

centers and then reabsorption by acceptors (radiative energy transfer). To distinguish the two processes, the time resolved fluorescence was further to be resolved in nanosecond and femtosecond time scale through TCSPC and femtosecond fluorescence upconversion method, respectively. Only a selection of these TCSPC measurements, which represent the typical decay for the dye-doped crystals, will be presented here. In Fig. 5, the TCSPC results from pure, tetracene- (1:24) and pentacene-doped (1:27) BSB-Me are plotted and fitted. By fitting analysis, the fluorescence decay at 480 nm for pure BSB-Me can be reproduced by a single exponential function with lifetime of 4.9 ns. When guest is doped into the BSB-Me, the data could no longer be fitted with a single exponential but biexponential decay, which indicates that there exists another decay process besides the spontaneous emission decay process, such as transfer of exciton energy of BSB-Me. From the results, it shows that the emission at 480 nm for doped BSB-Me decays faster than that of undoped composite, and both of the decay curves can be well fitted by a biexponential equation with the expression of [38]

$$I = (A_1 \exp(-t/\tau_1) + A_2 \exp(-t/\tau_2)) \times I_0 \quad (1)$$

where I and I_0 are the luminescence intensities at time t and 0, A_1 and A_2 are fitting constants, and τ_1 and τ_2 are the fast and slow decay time (luminescent lifetime), respectively.

The effective average lifetime τ of BSB-Me in doped crystals can be estimated by the following equation:

$$\tau = (A_1\tau_1^2 + A_2\tau_2^2)/(A_1\tau_1 + A_2\tau_2) \quad (2)$$

These results are summarized in Table 1.

The femtosecond fluorescence upconversion method was employed to obtain further insight on the dynamics of energy transfer, as shown in Fig. 6. We focused on the first 500 ps time window of the fluorescence intensity at short and long wavelengths. A clear slow rise with a rise time of ~100 ps is observed in the dynamics at the long wavelength (530 nm) for BSB-Me/tetracene crystals, and a more longer rise time (~280 ps) for BSB-Me/pentacene crystals. These slow rises of the fluorescence indicate that the species responsible for the emission at long wavelengths are mainly excited gradually during a time period much longer than the duration of the excitation pulse. Additionally, the rise time of the fluorescence is quite equal to the fast decay time of the fluorescence at short wavelengths (460 nm). It exhibits a more clearly evident of energy transfer process in doped crystal systems. The fact that the decay of the BSB-ME's fluorescence becomes rapid when energy transfer occurs is an indication of a nonradiative Förster energy transfer.

In the Förster transfer, the rate of energy transfer from a donor to an acceptor k_{ET} is given by

$$k_{ET} = \tau_0^{-1} \times (R_0/R)^6 \quad (3)$$

where τ_0 is the fluorescence lifetime of the pure donor system and R is the intermolecular separation of donor and acceptor. R_0 is Förster radius, which is intermolecular separation at which energy transfer competes equally with all other decay routs, and is proportional to the spectral overlap of the emission of donor and absorption of the acceptor. The transfer rate k_{ET} can be calculated from the decay times measured in the absence (τ_0) and presence of acceptor (τ_{DA}): $k_{ET} = 1/\tau_{DA} - 1/\tau_0$. For tetracene- (1:24) and pentacene-doped BSB-Me (1:27), the k_{ET} is equal to $2.03 \times 10^{10}\ s^{-1}$ and $5.58 \times 10^{10}\ s^{-1}$, respectively. And the energy transfer efficiency is 49.7% and 73.1%, respectively.

The investigated dynamics mentioned above are all under a low excitation density. It is known that high excitation intensity often cause appearance of nonlinear processes. All These processes may significantly influence operation of the devices [39–41]. The exciton dynamics for pure crystals and doped system at high excitation density are investigated, as shown in Fig. 7. The exciton dynamics is strongly intensity dependent, with faster decays observed for higher excitation levels. When the excitation is 4.9 μw, there is about fast decay component with about 28 ps, as illustrated in Fig. 7a. This behavior is

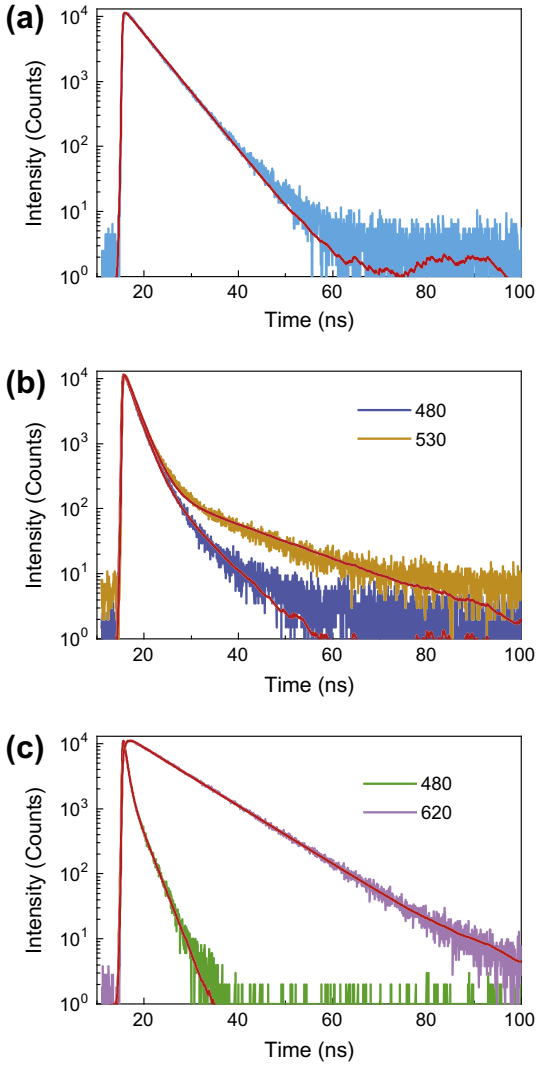

Fig. 5. Nanosecond fluorescence decays from pure, tetracene, and pentacene doped BSB-Me crystals.

Table 1
Decay data of pure BSB-Me crystal, tetracene-doped, and pentacene-doped BSB-Me crystals.

Sample	Decay time τ (ns)	Percentage (%)	Average lifetime τ (ns)	Transfer efficiency[a] (%)
BSB-Me	4.88	100	4.88	–
TE:BSB-Me	1.98 6.01	95.8 4.2	2.45	49.7
PE:BSB-Me	0.61 2.34	84.9 15.1	1.31	73.1

[a] The energy transfer efficiency is given by $E = k_{ET}/(1/\tau_0 + k_{ET}) = 1 - \tau_{DA}/\tau_0$.

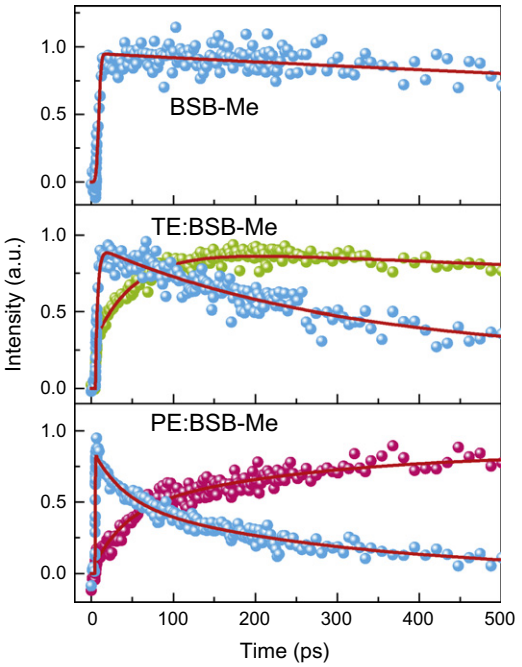

Fig. 6. Sub-picosecond fluorescence decays from pure, tetracene, and pentacene doped BSB-Me crystals.

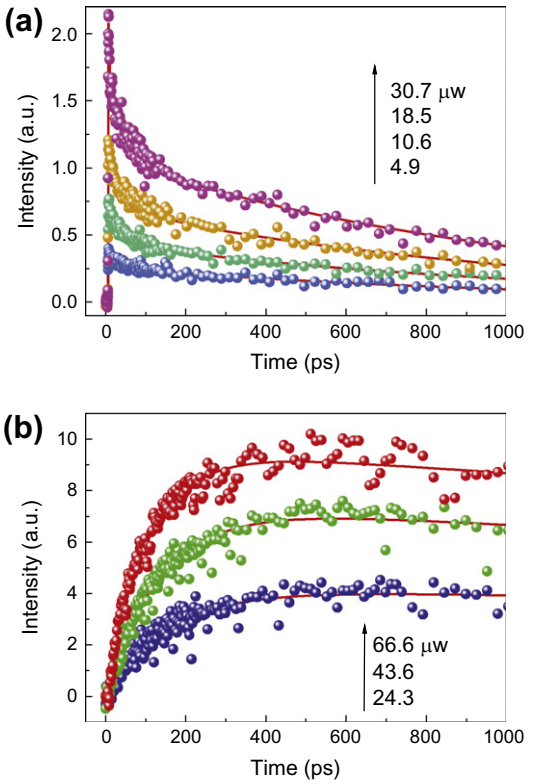

Fig. 7. Excitation intensity dependent emission dynamics of (a) pure and (b) pentacene-doped crystals monitored at wavelength of 480 nm and 620 nm, respectively.

similar as that in other solid-state organic materials. It possibly arises from the bimolecular deactivation processes due to exciton annihilation. At high excitation densities, the concentration of excitons generated after the photoexcitation is high, excitons will interact with each other and a pair of annihilation excitons may fuses to form a higher energy exciton. The dominant relaxation pathway of the high-energy exciton is found to be the internal conversion to the lowest excited state; so one excition is lost per interaction. The loss of excitons to annihilation is dependent on the excitation density and results in a faster decay of the fluorescence at higher excitation density. On the basis of their intensity dependence, we attribute the 28 ps decay component to annihilation of two excitons. At higher excitation intensities, when three excitations per complex are created, the annihilation becomes correspondingly faster and we can attribute a 3 ps relaxation component to a three-exciton annihilation when excitation is at 30.7 μw. In the doping BSB-Me samples, charge transfer processes may further quench the fluorescence. For the pentacene doped BSB-Me crystal (Fig. 7b), the kinetics exhibits much less excitation intensity dependence than that of the pure BSB-Me, indicating that the Förster energy transfer becomes the dominating process in the doping crystals.

4. Conclusions

We have prepared crystals of BSB-Me crystals doped with tetracene and pentacene. The RGB fluorescence emission can be achieved through doping technique. Both the steady-state fluorescence spectra and time-resolved fluorescence measurements indicate highly efficient energy transfer from the host BSB-Me to the acceptor molecules. Excitation intensity-dependent ultrafast dynamic shows that the kinetics in doped crystals exhibit much less excitation intensity dependence than that of the pure BSB-Me

crystals. Our results are relevant to the understanding of ultrafast energy-transfer dynamics in doped crystals and hence to development of novel organic optoelectronic devices.

Acknowledgements

The authors gratefully acknowledge the supports from National Basic Research Program of China (973 Program) under Grant No. 2011CB013005, and from Natural Science Foundation of China (NSFC) under Grant Nos. 90923037 and 61177024.

References

[1] K. Sakakibara, J.P. Hill, K. Ariga, Small 7 (2011) 1288–1308.
[2] K. Ariga, Q.M. Ji, J.P. Hill, Y. Bando, M. Aono, NPG Asia Mater. 4 (2012) e17.
[3] D. Natali, M. Caironi, Adv. Mater. 24 (2012) 1357–1387.
[4] H.L. Dong, H.F. Zhu, Q. Meng, X. Gong, W.P. Hu, Chem. Soc. Rev. 41 (2012) 1754–1808.
[5] M. Muccini, W. Koopman, S. Toffanin, Laser Photonics Rev. 6 (2011) 258–275.
[6] H.H. Fang, R. Ding, S.Y. Lu, X.L. Zhang, J. Feng, Q.D. Chen, J. Mater. Chem. 22 (2012) 24139–24144.
[7] D.P. Yan, A. Delori, G.O. Lloyd, T. Friscic, G.M. Day, W. Jones, J. Lu, M. Wei, D.G. Evans, X. Duan, Angew. Chem. Int. Edit. 50 (2011) 12483–12486.
[8] C. Reese, M.E. Roberts, S.R. Parkin, Z.A. Bao, Adv. Mater. 21 (2009) 3678–3681.
[9] C. Grivas, M. Pollnau, Laser Photonics Rev. 6 (2012) 419–462.
[10] P. Del Carro, A. Camposeo, L. Persano, S. Tavazzi, M. Campione, A. Papagni, L. Raimondo, L. Silvestri, P. Spearman, R. Cingolani, D. Pisignano, Appl. Phys. Lett. 92 (2008) 063301.
[11] H.H. Fang, R. Ding, S.Y. Lu, J. Yang, X.L. Zhang, R. Yang, J. Feng, Q.D. Chen, J.F. Song, H.B. Sun, Adv. Funct. Mater. 22 (2011) 33–38.
[12] S. Hotta, T. Yamao, J. Mater. Chem. 21 (2011) 1295–1304.
[13] H.H. Fang, Q.D. Chen, J. Yang, L. Wang, Y. Jiang, H. Xia, J. Feng, Y.G. Ma, H.Y. Wang, H.B. Sun, Appl. Phys. Lett. 96 (2010) 103508.
[14] H.H. Fang, Q.D. Chen, J. Yang, H. Xia, Y.G. Ma, H.Y. Wang, H.B. Sun, Opt. Lett. 35 (2010) 441–443.
[15] H. Wang, F. Li, I. Ravia, B.R. Gao, Y.P. Li, V. Medvedev, H.B. Sun, N. Tessler, Y.G. Ma, Adv. Funct. Mater. 21 (2011) 3770–3777.
[16] J. Yang, H.H. Fang, R. Ding, S.Y. Lu, Y.L. Zhang, Q.D. Chen, H.B. Sun, J. Phys. Chem. C 115 (2011) 9171–9175.
[17] R. Ding, H.H. Fang, Y. Wang, S.Y. Lu, X.L. Zhang, L. Wang, J. Feng, Q.D. Chen, H.B. Sun, Org. Electron. 13 (2012) 1602–1605.
[18] E.M. Garcia-Frutos, E. Gutierrez-Puebla, M.A. Monge, R. Ramirez, P. de Andres, A. de Andres, R. Ramirez, B. Gomez-Lor, Org. Electron. 10 (2009) 643–652.
[19] L. Jiang, W.P. Hu, Z.M. Wei, W. Xu, H. Meng, Adv. Mater. 21 (2009) 3649–3653.
[20] H.H. Fang, R. Ding, S.Y. Lu, L. Wang, J. Feng, Q.D. Chen, H.B. Sun, Opt. Lett. 37 (2012) 686–688.
[21] S.Z. Bisri, T. Takenobu, Y. Yomogida, H. Shimotani, T. Yamao, S. Hotta, Y. Iwasa, Adv. Funct. Mater. 19 (2009) 1728–1735.
[22] C. Hunziker, S.J. Kwon, H. Figi, M. Jazbinsek, P. Gunter, Opt. Express 16 (2008) 15903–15914.
[23] S. Kena-Cohen, S.R. Forrest, Nat. Photonics 4 (2010) 371–375.
[24] T. Takenobu, S.Z. Bisri, T. Takahashi, M. Yahiro, C. Adachi, Y. Iwasa, Phys. Rev. Lett. 100 (2008) 066601.
[25] F. Sasaki, M. Mori, S. Haraichi, Y. Ido, Y. Masumoto, S. Hotta, Org. Electron. 11 (2010) 1192–1198.
[26] X.J. Li, Y.X. Xu, F. Li, Y.G. Ma, Org. Electron. 13 (2012) 762–766.
[27] W.J.M. Naber, M.F. Craciun, J.H.J. Lemmens, A.H. Arkenbout, T.T.M. Palstra, A.F. Morpurgo, W.G. van der Wiel, Org. Electron. 11 (2010) 743–747.
[28] H. Wang, F. Li, B.R. Gao, Z.Q. Xie, S.J. Liu, C.L. Wang, D.H. Hu, F.Z. Shen, Y.X. Xu, H. Shang, Q.D. Chen, Y.G. Ma, H.B. Sun, Cryst. Growth Des. 9 (2009) 4945–4950.
[29] H. Nakanotani, M. Saito, H. Nakamura, C. Adachi, Adv. Funct. Mater. 20 (2010) 1610–1615.
[30] L.T. Kang, Y. Chen, D.B. Xiao, A.D. Peng, F.G. Shen, X. Kuang, H.B. Fu, J.N. Yao, Chem. Commun. (2007) 2695–2697.
[31] F. Xiao, R. Chen, Y.Q. Shen, Z.L. Dong, H.H. Wang, Q.Y. Zhang, H.D. Sun, J. Phys. Chem. C 116 (2012) 13458–13462.
[32] J.H. Wu, Z.P. Guan, T.Z. Xu, Q.H. Xu, G.Q. Xu, Langmuir 27 (2011) 6374–6380.
[33] X.P. Li, Y. Qian, S.Q. Wang, S.Y. Li, G.Q. Yang, J. Phys. Chem. C 113 (2009) 3862–3868.
[34] A.D. Peng, D.B. Xiao, Y. Ma, W.S. Yang, J.N. Yao, Adv. Mater. 17 (2005) 2070–2073.
[35] Y.S. Zhao, H.B. Fu, F.Q. Hu, A.D. Peng, W.S. Yang, J.N. Yao, Adv. Mater. 20 (2008) 79–83.
[36] C. Zhang, Y.S. Zhao, J.N. Yao, New J. Chem. 35 (2011) 973–978.
[37] C.F. Wu, Y.L. Zheng, C. Szymanski, J. McNeill, J. Phys. Chem. C 112 (2008) 1772–1781.
[38] J.R. Lakowicz, Principles of Fluorescence Spectroscopy, thirrd ed., Springer, New York, 2006.
[39] J.M. Hodgkiss, S. Albert-Seifried, A. Rao, A.J. Barker, A.R. Campbell, R.A. Marsh, R.H. Friend, Adv. Funct. Mater. 22 (2012) 1567–1577.
[40] A. Rao, M.W.B. Wilson, S. Albert-Seifried, R. Di Pietro, R.H. Friend, Phys. Rev. B 84 (2011) 195411.
[41] H. Wang, H.Y. Wang, B.R. Gao, L. Wang, Z.Y. Yang, X.B. Du, Q.D. Chen, J.F. Song, H.B. Sun, Nanoscale 3 (2011) 2280–2285.